Original Article

Hardfacing of mild steel with wear-resistant Ni-based powders containing WC particles using PPTAW technology

Augustine Appiah[1]* , Oktawian Bialas[1] , Marcelina Jędrzejczyk[2], Natalia Ciemała[2], Łucja Wantuch[2], Marcin Żuk[3] , Artur Czupryński[3] , Marcin Adamiak[1]

[1] Laboratory of Materials Research, Faculty of Mechanical Engineering, Silesian University of Technology, Gliwice, Poland; oktawian.bialas@polsl.pl (O.B.); marcin.adamiak@polsl.pl (M.A.)
[2] Student of the Faculty of Mechanical Engineering, Silesian University of Technology, Gliwice, Poland
[3] Department of Welding Engineering, Faculty of Mechanical Engineering, Silesian University of Technology, Gliwice, Poland; marcin.zuk@polsl.pl (M.Z.); artur.czuprynski@polsl.pl (A.C.)

*Correspondence: augustine.appiah@polsl.pl (A.A.)

Abstract: This study explores the use of powder plasma transferred arc welding (PPTAW) as a surface layers deposition technology to form hardfaced coatings to improve upon the wear resistance of mild steel. Hardfaced layers/coatings were prepared using the PPTAW process with two different wear-resistant powders: PG 6503 (NiSiB+60% WC) and PE 8214 (NiCrSiB+45% WC). By varying the PPTAW process parameters of plasma gas flow rate (PGFR) and plasma arc current, hardfaced layers were prepared. Microscopic examinations were carried out to investigate the microstructure and surface characteristics of the prepared hardfaced layers. Penetration tests were performed to ascertain the number and depth of crack sites in the prepared samples by visual inspection. The hardness of the hardfaced layers were determined: hardfacings prepared with PG 6503 had hardness of 46.3 – 48.3 HRC, those prepared with PE 8214 had hardness of 52.7 – 58.3 HRC. The microhardness of the matrix material was in the range of 573.3 – 893.0 HV, and the carbides had microhardness in the range of 2128.7 – 2436.3 HV. Abrasive wear resistance tests were carried out on each prepared sample to determine their relative abrasive wear resistance relative to the reference material, abrasion resistant heat-treated steel, Hardox 400, having a nominal hardness of approximately 400 HV. Findings from the research showed that the wear resistance of the mild steel was improved after deposition of hardfaced layers; the hardness and wear resistance were increased upon addition of Cr as an alloying element; increasing the PGFR increased the hardness and wear resistance of the hardfacings, as well as increase in the number of cracks; increasing the PTA current resulted in hardfacings with less cracks, but relatively lowered the wear resistance. The wear mechanisms were discussed.

Keywords: Plasma Transferred Arc method; abrasive wear; plasma cladding

Introduction

Metallic materials in use tend to degrade with time and eventually lose their usefulness. Conditions such as corrosion, creep, and wear, contribute to the failure of these materials. Studies have shown that most of these failure mechanisms originate from the surface of the material and an effective way of solving such problems is using surface treatment technologies as physical vapor deposition (PVD), chemical vapor deposition (CVD), thermal spraying, laser cladding (LC), and plasma transferred arc welding (PTAW)[1]. Surface engineering technologies have had a widespread use in several engineering disciplines including construction, power, automotive, etc. [2]. At the required substrate surfaces, deposition technologies are being used to develop advanced functional properties such as corrosion-resistant, wear-resistant, mechanical, magnetic, electrical, and optical properties [3]. All types of materials including metals, polymers, ceramics, and composites can be deposited onto similar or dissimilar materials. These technologies also allow for the formation of coatings of advanced engineering materials, metamaterials, multicomponent deposits, graded deposits, etc. Deposition technologies are used to alter the chemical and physical properties as well as the morphology of the surface of the substrate.

Surface treatment provides strategic ways of saving materials as well as aids in the design of components with desirable surface properties. This serves as a cheaper alternative to using conventional

materials to serve similar surface treatment purposes in large scale production. Plasma Transferred Arc Welding (PTAW), however, has been identified as an effective technology that can be used to overcome the surface treatment limitations such as dilution and poor adhesion, existing in other hardfacing technologies [4]. The PTAW technique has been in application since 1962, a time when the technology was used to modify materials surfaces by producing overlays [5]. In this technique, a plasma arc is created and confined around an electrode (e.g., tungsten (W) electrode), which is placed in a torch and mostly used as the cathode. The powder to be deposited is injected into the plasma in the presence of a shielding gas onto the substrate or workpiece, which is the anode. This shielding gas helps to prevent melting of the powder particles against oxidation [6]. Plasma arc has a high ionization, and this enables it to be fine-tuned to obtained desired results with regards to penetration and dilution. PTAW generally results in surface overlays of very high quality [7]. Relative to other methods of surface layers deposition, PTAW has many advantages. PTAW technique results in an improved adhesion between the overlays and the substrate. The energy flux associated with PTAW has a high stability. This technique has a relative higher melting efficiency [8]. The cost associated with PTAW welding implementation is relatively lower, while maintaining a relatively higher deposition efficiency [9]. The filler material for PTAW could either be in the form of a wire (called Plasma Arc Welding (PAW)) or powders (called Powder Plasma Arc Welding (PPTAW)). However, the powders are widely used in application, making heat demands for melting low [10]. The properties of the overlays produced from PPTAW depend primarily on the powder material used. However, the process parameters also contribute to the quality of the overlays. The most significant process parameters for wear resistant applications are the plasma gas flow rate (PGFR) and plasma arc current [11]. Industrial applications of PPTAW technology have increased over the years, mainly due to its compatibility of use with different powder materials. Most industrial uses of this technology are for abrasive resistance, corrosion resistance, and wear resistance. Some advanced industrial applications of PPTAW include the production of self-lubricating surfaces, and high temperature wear resistance [12]. PPTAW is used to address materials failure challenges in industries such as marine, ore mining, petrochemical, oil drilling, steel manufacturing, power generation, etc. [13].

This study explores the potential of PPTAW technology, using the powders of wear-resistant materials to prepare hardfaced layers to improve the wear resistance of mild steel plate.

## Materials and Methods

Sample Preparation

The main process for preparing the samples used in this work was PPTAW process. The sample preparation was carried out using the EuTronic© Gap 3511 DC synergic system at Castolin Eutectic© workshop in Gliwice, Poland. The PPTAW process parameters that were considered for preparing various samples are PGFR, plasma arc current, and torch travel speed. Two different groups of samples were prepared using two different wear resistant powders for the PPTAW hardfaced layers. The base/substrate material used was a mild steel plate with the dimensions of 94 mm X 30 mm X 10 mm, shown in Fig. 1 (a). The powders were obtained from Castolin Eutectic© PG 6503 and PE 8214. PG 6503 consists of the NiSiB matrix with 60%WC and PE 8214 consists of the NiCrSiB matrix with 45%WC. Eight (8) samples were prepared in total; four (4) for each powder, with varying PTAW process parameters. To obtain the desired microstructure and mechanical properties of a hardfaced layer, selection of optimal PPTAW process parameters is an important step. The most reliable hardfaced layers are those configured and prepared to have the least surface defects, high rate of deposition, less distortion as well as low dilution [14]. The PPTAW process parameters – PGFR and plasma arc current – were varied to obtain information on their effects on the structure and properties of the hardfaced layers. Additionally, variation of these process parameters provides control over the PPTAW process for easier reproducibility of hardfaced layers with superior wear-resistant properties. The parameters for preparing the layers are given in Table I. The thickness of the hardfaced layers on the surface of the substrate material varied slightly, in the range of 2.3 mm, for PE-5 to 3.0 mm, for PG-2, as the process parameters were adjusted. This is illustrated in Fig. 1 (b). The prepared hardfaced layers on the surface of mild steel are also shown in Fig. 2.

**Table I.** PTAW parameters for sample preparation

| Coating/Sample ID	Powder used	Current (A)	Travel speed, V (mm/s)	PGFR (l/min)
PG-1	PG 6503	110	1.3	1.2
PG-2	PG 6503	150	1.3	1.2
PG-3	PG 6503	110	1.3	1.0
PG-4	PG 6503	110	1.3	1.5
PE-5	PE 8214	110	1.3	1.2
PE-6	PE 8214	150	1.3	1.2
PE-7	PE 8214	110	1.3	1.0
PE-8	PE 8214	110	1.3	1.5

(a)

(b)
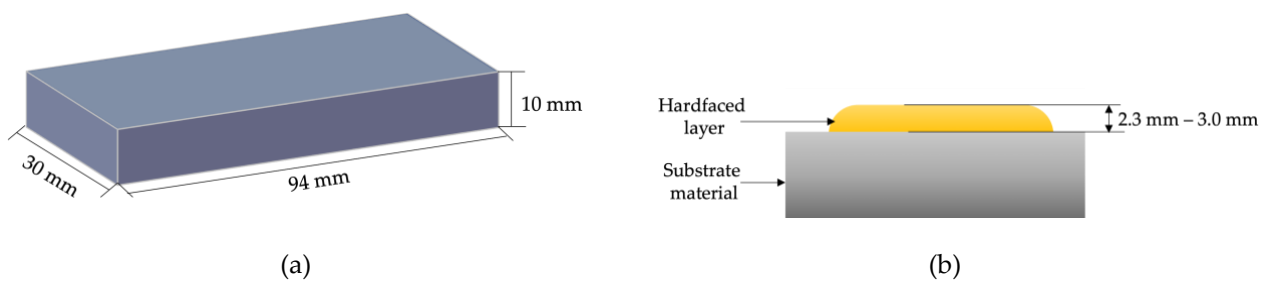
Fig. 1. Schematic diagrams showing the dimensions of the prepared samples (a) dimensions of the prepared mild steel plate to be used as substrate material (b) cross-section of the final material after deposition of the hardfaced layer onto the substrate material, showing the range of thickness of the hardfaced layers for the various samples
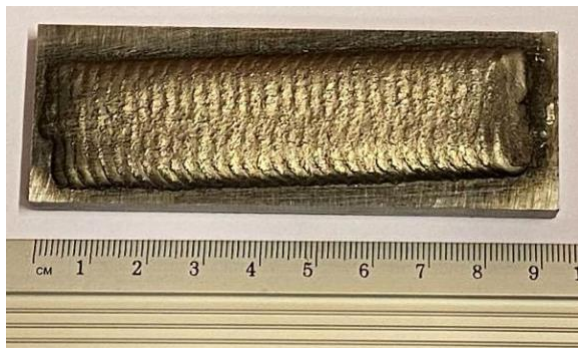
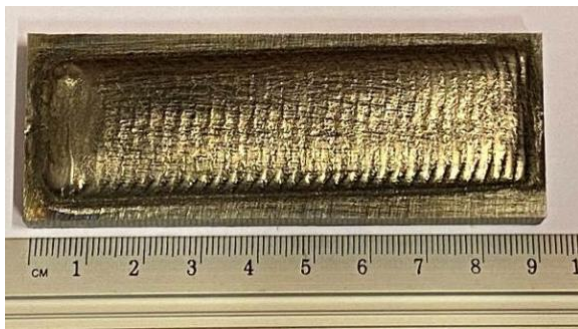PG 6503 - 110 A, 1.3 mm/s, 1.2 l/min
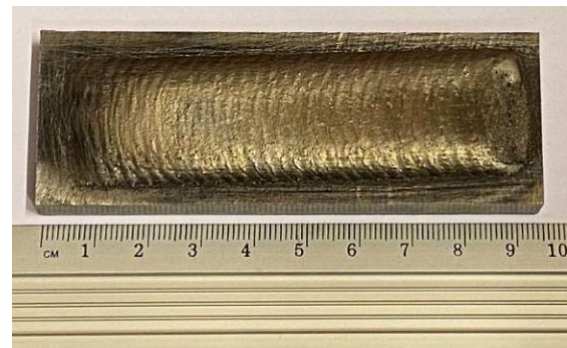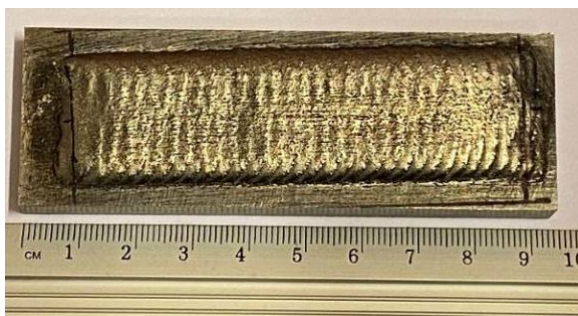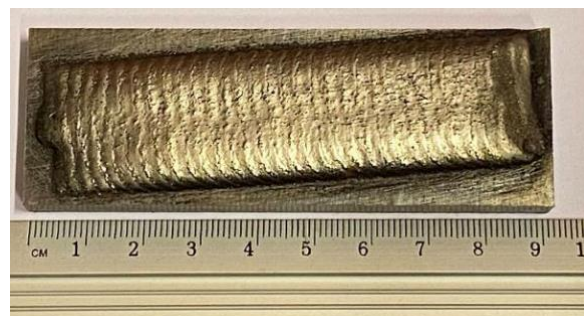
(a)

PG 6503 - 150 A, 1.3 mm/s, 1.2 l/min

(b)

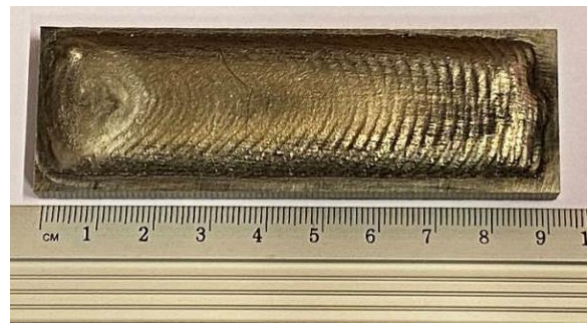PG 6503 - 110 A, 1.3 mm/s, 1.0 l/min

(c)

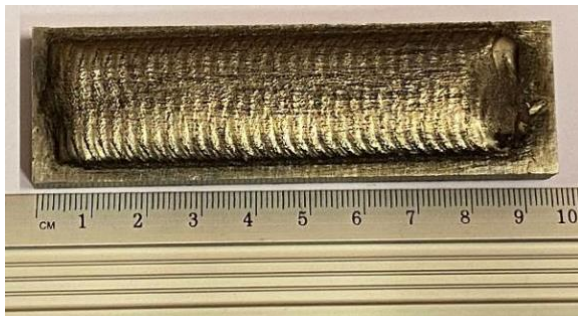PG 6503 - 110 A, 1.3 mm/s, 1.5 l/min

(d)

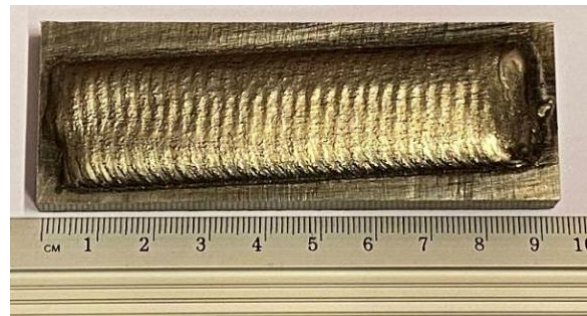PE 8214 - 110 A, 1.3 mm/s, 1.2 l/min

(e)

PE 8214 - 150 A, 1.3 mm/s, 1.2 l/min

(f)

PE 8214 - 110 A, 1.3 mm/s, 1.0 l/min

(g)

PE 8214 - 110 A, 1.3 mm/s, 1.5 l/min

(h)

Fig. 2. Images of prepared hardfaced layers on the surface of substrate material (a) PG-1 (b) PG-2 (c) PG-3 (d) PG-4 (e) PE-5 (f) PE-6 (g) PE-7 (h) PE-8

Characterization and Testing

Scanning electron microscopy (SEM) was performed using Supra 35 (ZEISS, Oberkochen, Germany) to obtain the micrographs of the powder morphology. Digital images of the prepared samples were taken by the Leica DVM6 digital microscope (Leica Microsystems AG, Switzerland) to obtain information on the surface porosity and crack development. The micrographs of the microstructure of the prepared hardfaced coatings were obtained using the light microscope AxioVision (ZEISS, Jena, Germany).

Penetration test was carried out to identify cracks that had been developed in the hardfaced layer after the PPTAW hardfacing process. This test was carried out based on the specifications of PN-EN ISO 3452 standard. The test proceeded with the use of MR® 70 developer, MR® 79 remover (acetone) and MR® 68NF penetrant. For each specimen, the surface was first cleaned thoroughly with acetone to get rid of impurities. The surface was then sprayed with the penetrant and allowed to dry for 10 -15 minutes. The penetrant was then cleaned from the surface with the help of the remover and paper. The surface of the sample was then sprayed with the developer and allowed to settle for some time. After that, it would be observed that the penetrant begun to appear on the surface of the specimen, from the sites where cracks exist.

The metal-mineral abrasive wear resistance test of the as-deposited hardfaced layers as well as the reference material (abrasion resistant steel grade AR400) was carried out according to the procedures outlined in ASTM G65-00. This abrasive wear testing method called "rubber wheel" according to the ASTM G65 standard has been the most used test in materials engineering for assessing the metal-mineral abrasive wear resistance. Quartz sand was used in the test as the abrasive, with a grain size of 50 – 70 mesh (0.297 – 0.210 mm); and fed to the friction zone gravitationally. With regards to the PTAW hardfaced layer and the reference material, the experimental test involved the preparation of two specimens with dimensions 75 mm x 25 mm x 10 mm. The rubber wheel made 6000 revolutions in approximately 30 minutes of the test. A pressure force of 130N was applied to the material. The feed rate of the abrasive (A.F.S. Testing Stand 50-70 mesh) was 335 g/min.

The weights of the specimens were taken before and after the abrasive wear test on the balance in the laboratory which has an accuracy of up to 0.0001g. The average density of the hardfaced layer and that of the reference material were determined from three measurements of the density of the specimen, sampled

and weighed at room temperature in air and liquid. The volume loss was calculated from the measured average density of the hardfaced layer and the average mass loss after abrasion using the equation below.

$$\text{Volume loss [mm}^3] = \frac{\text{mass loss [g]}}{\text{density [g/(cm}^3)]} \times 1000 \qquad (1)$$

   The Archimedes method, according to ISO ASTM D792 standard, was used to measure the density of the hardfaced layer. A Radwag AS 220.R2 analytical laboratory balance (Radwag, Warsaw, Poland) was used in the measurement along with a set for Archimedes-method-based density measurements.
   The microhardness of the hardfaced layers were tested using the microhardness tester FM-ARS 9000 (Future-Tech Corp., Tokyo, Japan) to obtain the Vickers hardness with a load of 1kg. The hardness values of the matrix were determined by measuring the hardness in a cross-sectional manner from the surface of the coating to the substrate with 0.3mm between each point. The surface hardness was measured with a Rockwell hardness tester SHR-1500E (Guizhou Sunpoc Tech Industry Co., Ltd., Guiyang City, China) with a load of 150kg, to determine effects of the different process parameters on the hardness of the prepared hardfaced layers.

Results

Visualisation of scanning electron microscopy of the powders morphology
   The significance of metal matrix composites (MMC) powders is greatly influenced by the shape of the powder particles. Angular shaped powders are mostly preferred in wear-resistant applications, whereas spherical shaped powders are desirable in high toughness applications. A balance of these morphologies however, results in a more mechanically balanced material that is suitable for applications requiring corrosion resistance, high hardness, high toughness, and wear resistance [15]. The morphology of the powders used in the PPTAW process was obtained by scanning electron microscopy. The images obtained from this analysis are presented in Fig. 3 and Fig. 4. The SEM images show a mix morphology of spherical and angular shaped powders. The matrix powder particles had spherical shapes, whiles the WC particles appeared with sharp-edged angular morphology.
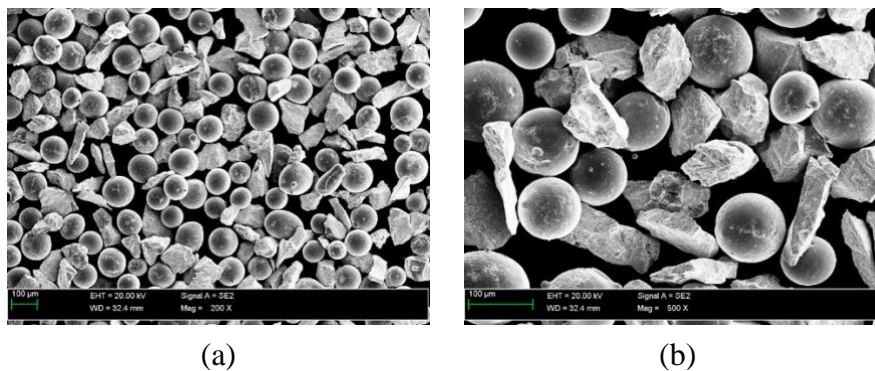

(a)   (b)

Fig. 3. SEM images of PE 8214 powders; (a) 200x; (b) 500x
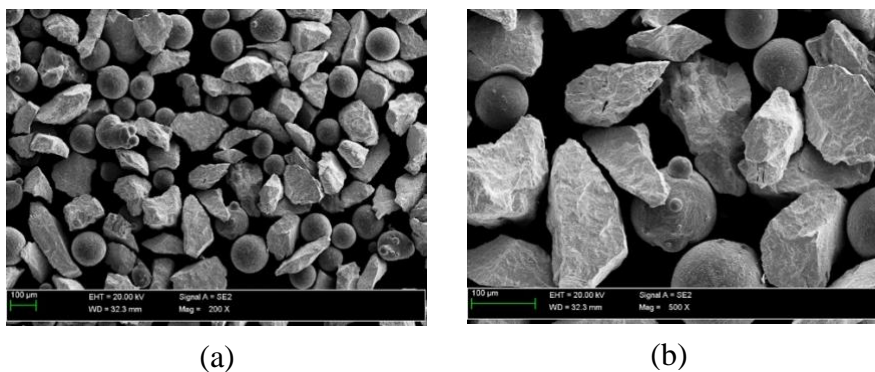

(a)   (b)

Fig. 4. SEM images of PG 6503 powders; (a) 200x; (b) 500x

Microstructure of prepared samples

Considering the strong direct relationship between the structure and properties of materials, it was necessary to examine the microstructure of the prepared samples under the various conditions of preparation. The obtained micrographs, at a magnification of 500X, provide information on the dissolution of the WC particles in the Ni-based alloyed matrices under the various conditions of varying PPTAW process parameters – PGFR and PTA current. These micrographs are shown in Fig. 5.

When the plasma gas flow rate (PGFR) was increased to 1.2 L/min (Fig. 5a) from 1.0 L/min (Fig. 5c), the carbides are seen in the matrix with softer edges, indicating a degree of dissolution into the matrix. When the PGFR was further increased to 1.5 L/min (Fig. 5d), there is still seen this same level of dissolution as seen when the PGFR was 1.0 L/min (Fig. 5c). The level of dissolution of the carbides into the matrix was significantly seen when the PGFR was increased from 1.0 L/min to 1.2 L/min. However, when the PGFR was increased from 1.2 L/min to 1.5 L/min, there was no observation of a significant level of dissolution between these PGFR values.
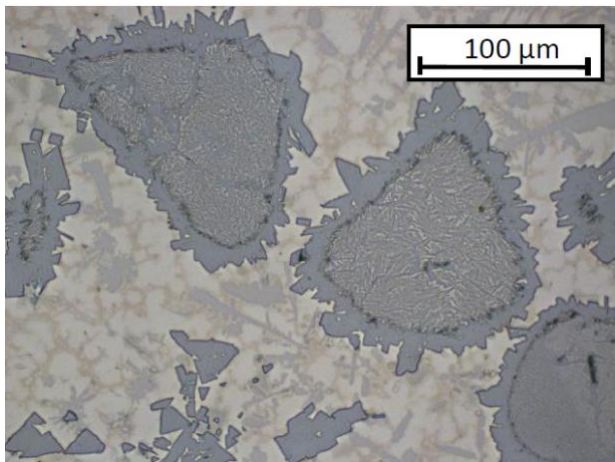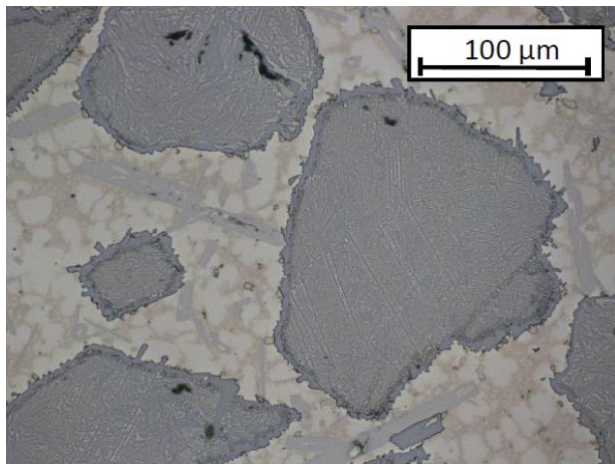

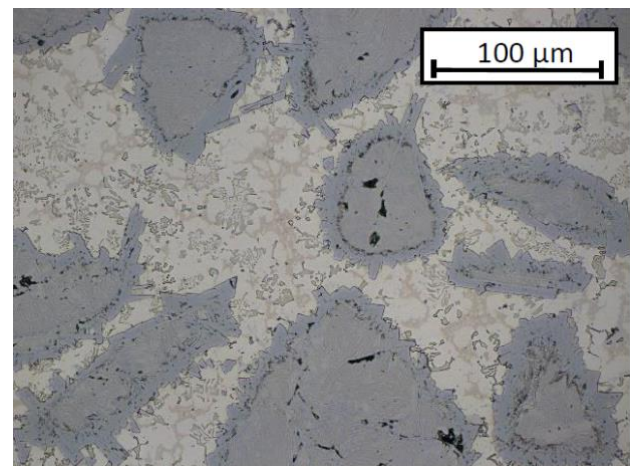PG 6503 - 110 A, 1.3 mm/s, 1.2 l/min
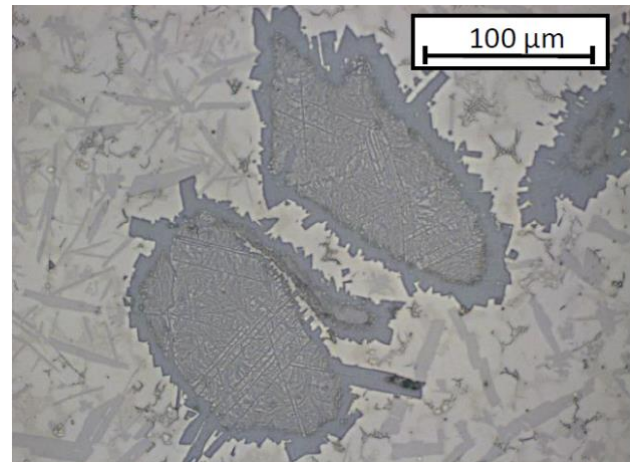
(a)

PG 6503 - 150 A, 1.3 mm/s, 1.2 l/min
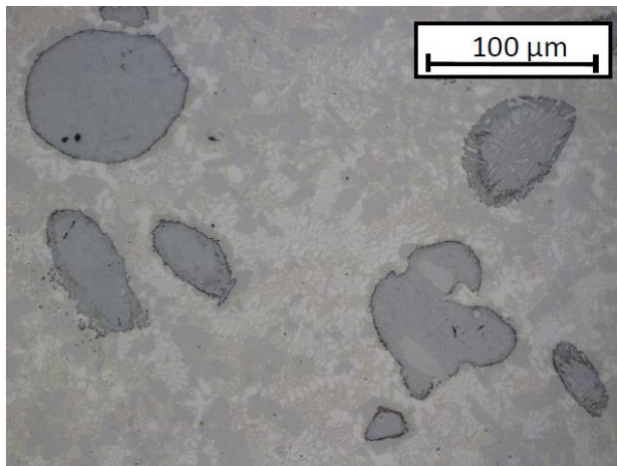
(b)

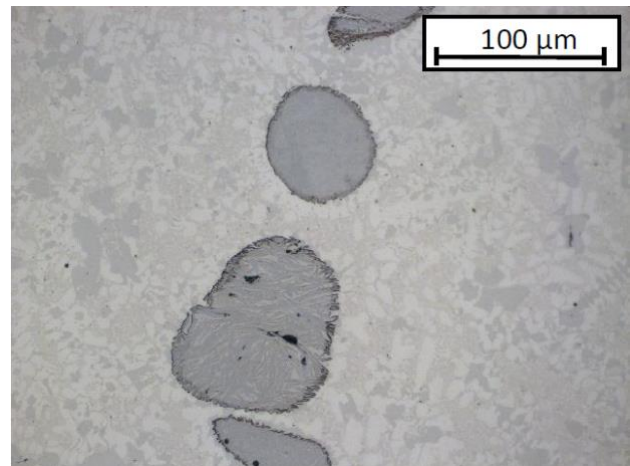PG 6503 - 110 A, 1.3 mm/s, 1.0 l/min
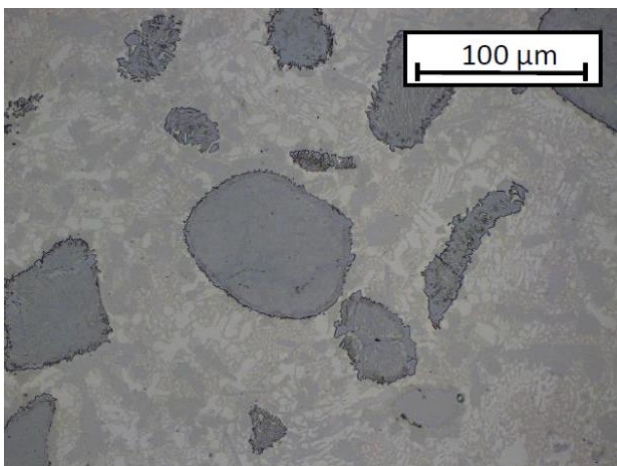
(c)

PG 6503 - 110 A, 1.3 mm/s, 1.5 l/min

(d)

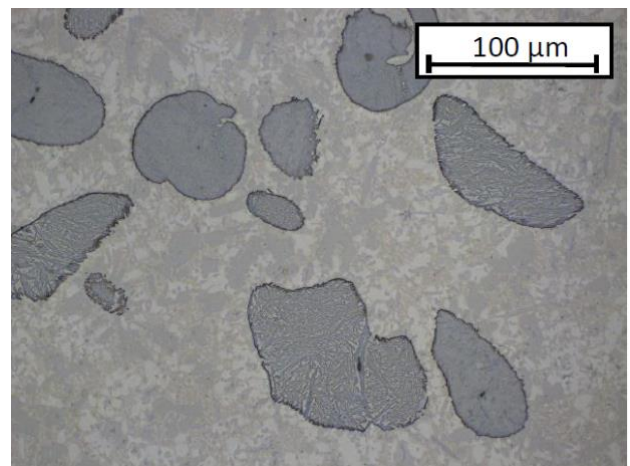PE 8214 - 110 A, 1.3 mm/s, 1.2 l/min

(e)

PE 8214 - 150 A, 1.3 mm/s, 1.2 l/min

(f)

PE 8214 - 110 A, 1.3 mm/s, 1.0 l/min

(g)
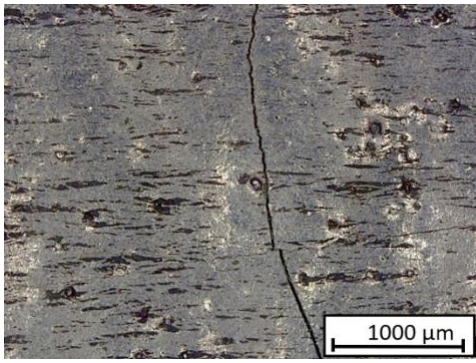
PE 8214 - 110 A, 1.3 mm/s, 1.5 l/min

(h)

Fig. 5. Micrographs of the prepared samples at 500X magnification (a) PG-1 (b) PG-2 (c) PG-3 (d) PG-4 (e) PE-5 (f) PE-6 (g) PE-7 (h) PE-8

Similarly for layers prepared with powder PE 8214, it is observed from the micrographs that the increase in the PGFR from 1.0 L/min (Fig. 5g) to 1.2 L/min (Fig. 5f), resulted in an observation of a slight dissolution of the carbides into the matrix. As the PGFR was increased further to 1.5 L/min (Fig. 5h), there is no longer seen enough dissolution of the carbides into the matrix. Generally, increasing the PGFR increased the degree of dissolution of the carbide particles into the matrix. Also, as the current was increased, the degree of dissolution of the carbides into the matrix was seen to increase slightly. Although this dissolution is not dramatic, the edges of the carbides when the current was 150A (Fig. 5b, and 5f), were less sharp compared to when the current was 110A (Fig. 5a and 5e).

Crack sites in the coatings

The formation of cracks, as well as their origin and propagation were investigated using digital microscopy. Information regarding the depth of the cracks was also investigated in a penetration test using the guidelines outlined in the PN-EN ISO 3452 standard. Images from the digital microscopy and penetration tests are presented in Fig. 6 and Fig. 7, with details on surface crack development.
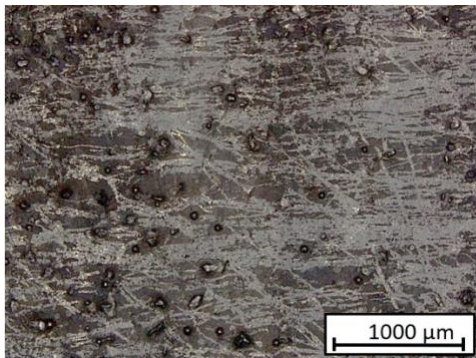
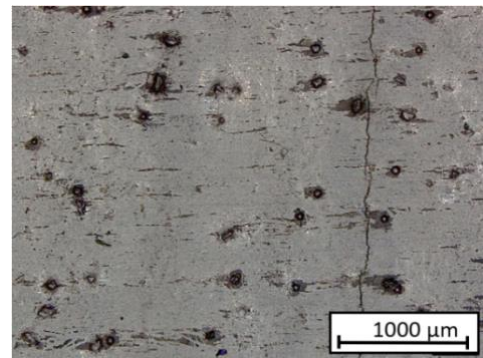PG 6503 - 110 A, 1.3 mm/s, 1.2 l/min
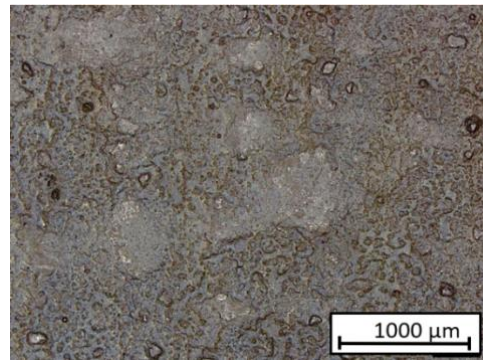
(a)

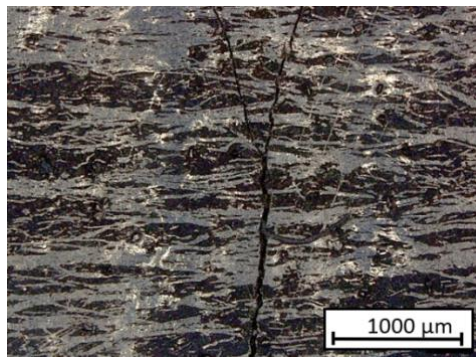PG 6503 - 150 A, 1.3 mm/s, 1.2 l/min

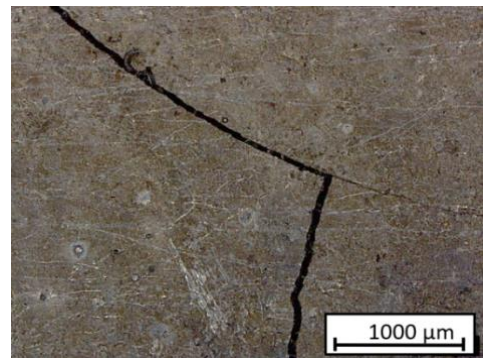(b)

PG 6503 - 110 A, 1.3 mm/s, 1.0 l/min

(c)

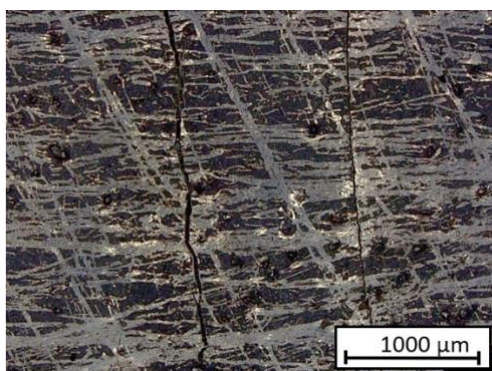PG 6503 - 110 A, 1.3 mm/s, 1.5 l/min

(d)
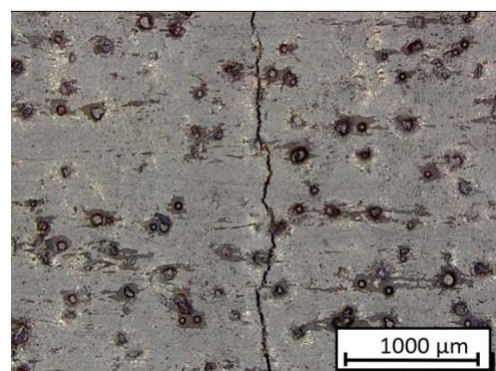
PE 8214 - 110 A, 1.3 mm/s, 1.2 l/min

(e)

PE 8214 - 150 A, 1.3 mm/s, 1.2 l/min

(f)

PE 8214 - 110 A, 1.3 mm/s, 1.0 l/min
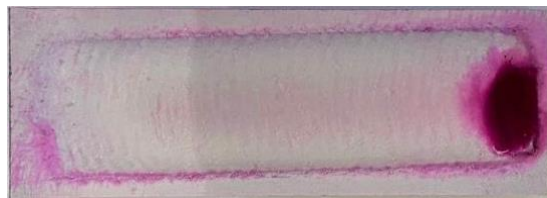
(g)

PE 8214 - 110 A, 1.3 mm/s, 1.5 l/min

(h)

Fig. 6. Digital images of the surfaces of as-deposited hardfaced layers showing crack development and surface porosity, (a) PG-1 (b) PG-2 (c) PG-3 (d) PG-4 (e) PE-5 (f) PE-6 (g) PE-7 (h) PE-8
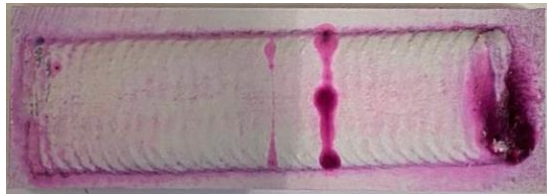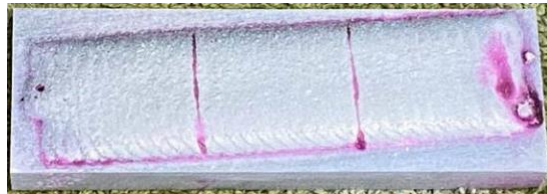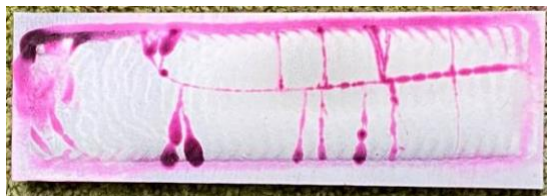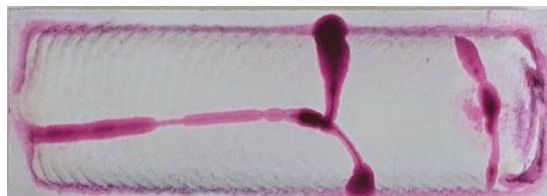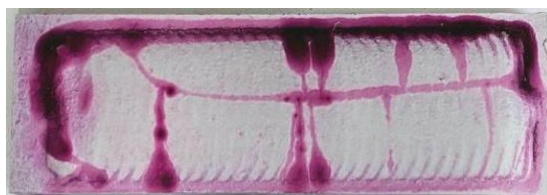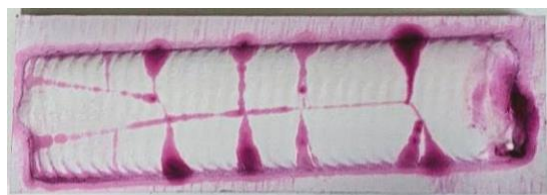
Fig. 7. Images of samples after penetration test showing the origin and depth of cracks on the surfaces of the hardfaced layers(a) PG-1 (b) PG-2 (c) PG-3 (d) PG-4 (e) PE-5 (f) PE-6 (g) PE-7 (h) PE-8

It was observed form both the digital microscopy and penetration tests that, the samples prepared with the powder PE 8214 had more cracks than the samples prepared with the powder PG 6503. The penetration test resulted in providing information on visible cracks that had been formed in the samples after preparation. As the PGFR was increased from 1.0 L/min to 1.2 L/min, there is no significant changes in the number of crack sites on the surface. However, when the PGFR was increased to 1.5 L/min, the number of crack sites were seen to increase. For all coatings prepared by both powders, there was a common observation that increasing the PTAW current, whiles keeping all other parameters equal, reduced the number of crack sites in the coatings.

Abrasive Wear Resistance

Abrasive wear resistance tests were carried out to investigate the metal-mineral abrasive wear performance of the prepared hardfaced layers against the abrasive resistant material Hardox 400 (AR400). The volume loss was estimated due to high difference between the density of WC and metallic matrix and the reference material. The abrasive wear resistance test results are presented in Table II. The relative abrasive wear resistance was computed against that of the reference material, AR400.

Table II. Results of the metal-mineral abrasive wear resistance tests concerning the surface layer PPTAW deposition of NiSiB+60%WC and NiCrSiB+45%WC composite powders on mild steel in comparison with the abrasive wear resistance of abrasion resistant steel AR400

| Sample ID	Mass before test, g	Mass After test, g	Mass Loss, g	Average Mass Loss, g	Material Density, g/cm³	Average volume loss, mm³	Relative Abrasive Wear Resistance*
PTAW Hardfaced Layer (NiSiB+60%WC)							
PG-1	228.6697	228.3604	0.3093	0.3093	11.1935	27.6321	4.8
PG-2	231.6575	230.8754	0.7821	0.7821	11.1935	69.8709	1.9
PG-3	226.4951	226.2412	0.2539	0.2539	11.1935	22.6828	3.1
PG-4	221.7090	221.2348	0.4742	0.4742	11.1935	42.3639	2.7
PTAW Hardfaced Layer (NiCrSiB+45%WC)							
PE-5	209.0038	208.7471	0.2567	0.2567	9.8274	26.1208	5.1
PE-6	196.0594	195.6905	0.3689	0.3689	9.8274	37.5378	3.5
PE-7	195.6418	195.3264	0.3154	0.3154	9.8274	32.0939	4.7
PE-8	227.8358	227.5979	0.2379	0.2379	9.8274	24.2078	5.5
Reference Material - AR400 Steel							
H1	104.6219	103.4971	1.1248	1.0318	7.7836	132.5607	1.0
H2	111.7377	110.7989	0.9388				

*Relative abrasive wear resistance is in relation to the abrasion-resistant steel AR400 .

The graph below shows the average volume losses of the specimen compared to that of the reference material (Ref.).
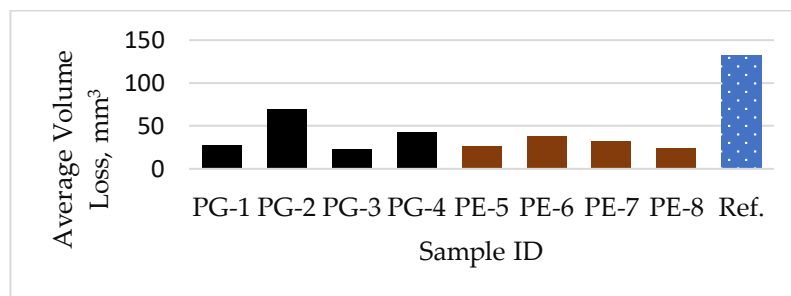
(a)
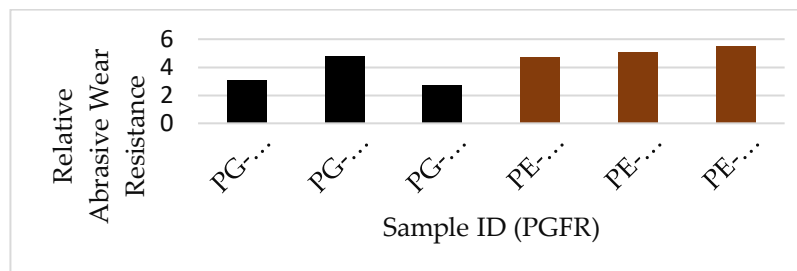
(b)

Fig. 8. (a) Graph showing how the average volume losses of the specimen compare to the average volume loss of the reference material (b) Relative abrasive wear resistance with changes in PGFR

When comparing the average volume losses of the specimen to the average volume loss of the reference material in Fig. 8 (a), the average volume losses of the samples prepared using the powder PG 6503 were relatively higher, with an average of 40.64 mm³ volume loss, than the average volume losses of the samples prepared using the powder PE 8214, which had an average of 29.99 mm³. It is seen in Fig. 8 (b) that for the samples prepared using powder PG 6503, the relative abrasive wear resistance increased with a slight increase in the PGFR but decreased significantly as the PGFR was further increased. Conversely, for the coatings prepared using the powder PE 8214, the relative abrasive wear resistance increased as the PGFR was increased. The samples prepared with the powder PE 8214 exhibited increase in the relative abrasive wear resistance with increasing PGFR from 1.0 L/min to 1.2 L/min, because more particles started melting into the matrix. For PE-8 which has a PGFR of 1.5 L/min, the level of porosity in the coating was relatively lower, which resulted in a higher relative abrasive wear resistance. The calculations of relative abrasive wear resistance in Table II, show that, in the case of the coatings prepared with powder PG 6503, the relative abrasive wear resistance significantly reduced as the current was increased from 110A in PG-1 to 150A in PG-2. Similarly, there was a reduction in the relative abrasive wear resistance in the coatings prepared with the powder PE 8214 when the current was increased from 110A in PE-5, to 150A in PE-6. The layers prepared with powders of PE 8214 exhibited higher relative abrasive wear resistance than those prepared with the powders of PG 6503.

Hardfaced Layer Hardness

The surface hardness was tested for the hardfacings to investigate the contributions of the various process parameters on the hardness of the surface. This was also used to investigate the effects of the heat affected zones (HAZ) on the microhardness of the layers. Table III shows the microhardness results for both the matrix and the carbides for the layers based on both powders. The results of the Rockwell C surface hardness test are presented in Table IV.

Table III. Microhardness across the cross-section of hardfaced layers

Sample ID	Microhardness of Matrix, HV		Microhardness of Carbides, HV	
	Mean	Standard Dev.	Mean	Standard Dev.
PG-1	573.3	10.2	2128.7	33.3
PG-2	687.0	2.4	2162.7	76.1
PG-3	590.7	5.2	2413.0	62.9
PG-4	673.0	18.5	2275.0	49.5
PE-5	844.7	23.2	2436.3	24.1
PE-6	888.7	23.8	2343.3	61.6
PE-7	888.7	18.0	2349.3	38.7
PE-8	893.0	16.1	2391.3	80.5

Table IV. Surface hardness of hardfaced layers

Sample ID		PG-1	PG-2	PG-3	PG-4	PE-5	PE-6	PE-7	PE-8
Rockwell C Hardness, HRC	Mean	47.3	47.7	46.3	48.3	52.7	55.3	58.3	55.7
	Standard Dev.	2.6	2.5	0.5	1.2	3.3	2.9	3.7	1.2

The measured microhardness as observed in the matrix, was seen to be high from the surface of the coating and when it gets into the interface, which is around 2.7 mm to 3.0 mm away from the surface, a decrease begins. This proceeds further and the lowest microhardness is seen in the substrate material. It is observed from Tables III and IV that the hardness values of the samples prepared by the powder PE 8214 (NiCrSiB+45%WC) were greater than the values of the samples prepared by the powder PG 6503 (NiSiB+60%WC), from the surfaces of the coatings and even at the interfaces. However, the values were seemingly the same in the substrate material. This observation of higher hardness in PE 8214 than PG 6503 can be explained by the presence of chromium in the powder PE 8214. In a study, Tian et. al., [16] investigated the effect of chromium content on the mechanical properties of an alloy. Findings from the study reported that increasing the chromium content in the alloy significantly increased the hardness and the wear resistance of the alloy.

Discussion

Effect of MMC powder particle morphology

The selection of the wear resistant powders used in this study was aimed at the morphological structure of the powder particles, as well as the effects of this morphology on the wear resistance of the produced hardfaced layers. The morphology of the powders used, under the SEM (Fig. 3 and 4), had a mixed morphology of spherical and angular shapes. In a study on the effects of WC powder particle morphology on the wear rate of surface coatings, Huang et. al., [17] reported that the wear resistance of the coating layer is influenced by a mean free distance which exists between WC particles, where even the slightest dissolution of the WC particles would have significant effects on the wear properties of the coating. This was observed because the hardfaced layers formed by spherical powder particles show relatively wider gaps between the reinforcement, which contrasts with the interlocking nature of the structure formed by the angular powder particles, reducing the contact between the abrasive particle and the matrix material [17]. This observation is supported in this study; as less WC particles are dissolved in Fig 5 (c) than in Fig 5 (d), the relative abrasive wear resistance correspondingly increased from PG-4 to PG-3, as reported in Table II.

Effects of PGFR on the mechanical properties of the hardfaced layers

The current state of PPTAW provides insight on how plasmas gas flow rate (PGFR) is a major contributing factor to the resultant mechanical properties of the hardfaced layer [18,19]. In this study, the effects of PGFR on the microstructure, hardness, abrasive wear resistance, crack formation and propagation, of the hardfaced layers were studied. An increase in the PGFR had a corresponding increase in the rate of dissolution of the particulate carbides into the matrix. This increase however was seen to be not significant as the PGFR values increased further. This observation can be explained by the presence of residual plasma gas in the plasma jet when the PGFR is high. This inhibits progressive heat dissipation and consequently prevents further dissolution of powder particles[20].

There was a direct relationship between the values of PGFR and the number of crack sites present in the hardfaced layer, for layers prepared from both powders. At higher values of PGFR, there is increased pore formation resulting from plasma gas that has been entrapped in the plasma jet. This entrapment results in inadequate melting of particles that have agglomerated and hence they exhibit low thermal conductivity, resulting in poor resistance to crack formation by the hardfaced layers.

The abrasive wear resistance exhibited by the layers prepared with the powder with composition NiCrSiB+45%WC (PE – 8214) was generally higher than that exhibited by the layers prepared with the powder NiSiB+60%WC (PG – 6504). This observation is particularly noticeable as the PGFR was increased in both situations and it can be attributed to the presence of chromium in the PE – 8214 powders. Alloying with Cr generally increases the wear resistance of materials [16]. El-Mahallawi et. al., [21] evaluated the effect of Cr in alloys by studying high manganese steel containing 1-7 and 2-3 wt% Cr. These steels were subjected to different wear conditions including abrasion, corrosion, and combined impact-abrasive wear. The performance of these Cr alloyed steels was compared to plain Hadfield steels, and it was reported that the Cr alloyed manganese steels had wear resistance superior to those of the Hadfield steels. This also supports the observation of an increase in the abrasive wear resistance as the PGFR was increased for samples prepared with this powder. The PGFR aids in introducing powder materials onto the surface of the substrate and as it increases, the more powders are deposited in the PPTAW process [20]. This increases overall the Cr content, with a corresponding increase in wear resistance. A similar outcome was observed in the study by Tian et. al., [16] on the effect of chromium content on microstructure, hardness, and wear resistance of as-cast Fe-Cr-B alloy. The Cr content was varied from 0wt% in incremental of 4wt% to 20wt%. It was reportedly observed that as the Cr content increased, the wear resistance and hardness also increased until reaching an equilibrium at 12wt% Cr, after which there was not much significant increase in these mechanical properties. Hardfaced layers prepared by both powders exhibited an increase in hardness when the PGFR was also increased. As the PGFR was increased, the plasma power correspondingly increased, resulting in a higher particle temperature. With an increased temperature of the particles, dissolution of the carbides into the matrix is accelerated. This enhances the adhesion between the particles, resulting in lower porosity and enhanced hardness [22].

Effects of PTA current on the mechanical properties of the hardfaced layers

Increasing the PPTAW process current resulted in higher degrees of dissolution of the carbides into the matrix, with corresponding reduction in crack formation, as well as the number of crack sites in the layered coatings. The surfaces of the coatings tend to be relatively smoother and with less cracks when the PTA current increases. This is because as the current increases, the particles absorb more energy, creating a rise in particle temperature, resulting in the eventual reduction in porosity of the system [15]. The state of stress in the padding weld is also affected by the amount of heat introduced into the material. The greater the amount of the supplied heat, the slower the rate of dissipation of heat from the material into the environment, resulting in a lower stress state and an eventual reduction in cracks [23].

A rise in the plasma arc current mostly results in an increase in the fraction of the base material in the padding weld, resulting in an increase in wear resistance [24]. In this work however, for both powders, the coatings formed had a reduction in the relative abrasive wear resistance when the current was increased from 110A to 150A. This is because it was observed that an increase in the PTA current increased the dissolution of the powder particles. This caused the surface to be relatively smoother with relatively shallow grooves on the surface as shown in samples PG-1 (Fig. 2a) and PG-2 (Fig. 2b). This relatively smoother surface and shallow surface grooves contribute to the reduction in the relative abrasive wear resistance of the coatings [25]. Adjusting the PTA current higher provides more energy to be absorbed by the powder particles, causing an increase in temperature. This results in reduction in porosity as the rate of dissolution of the powder particles increases with increasing PTA current. The relatively higher rate of particle dissolution and lower levels of porosity associated with an increase in the PTA current consequently results in the increase in the hardness of the coatings [26]. This is indicative of the higher microhardness values recorded in this study as the PTA current was increased. It is reported in Tables III and IV that as the PTA current was increased, there was a corresponding increase in the surface hardness as well as the depth of the microhardness across the cross-section of the layers. This is because the depth of the heat affected zone (HAZ) increases as the PTA current increases since there is a rise in the output heat of the plasma in this situation. Comparison of the size of the HAZ with increase in PTA is visualized in Fig. 9. Higher hardness is desirable in some applications, however, due to the growth of the HAZ as the PTA current is increased, producing the hardfaced layers at higher PTA current intensities is not encouraged. This is because the introduced heat results in a more brittle microstructure upon cooling, and this will significantly affect the toughness of the material and result in poor adhesion at the substrate-coating interface [27].
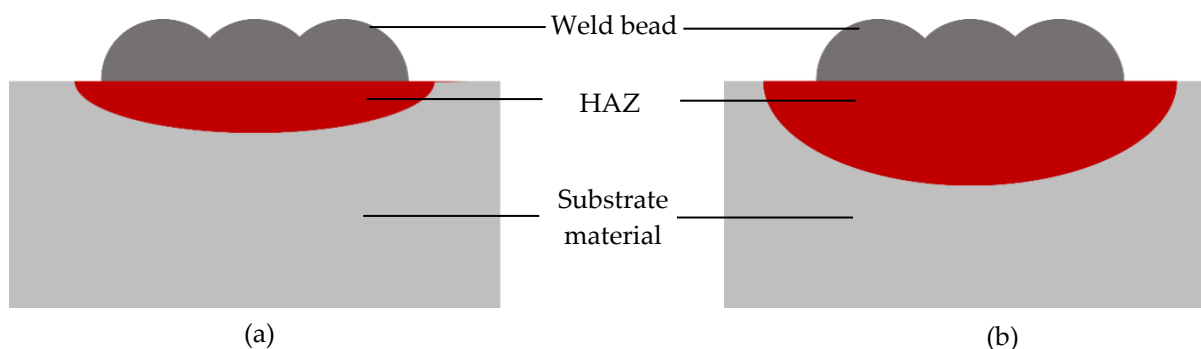

Fig. 9 Comparison of heat affected zones (HAZ) with an increase in PTA current (a) The HAZ is smaller with a lower value of PTA current at 110A (b) The HAZ is relatively larger with an increased value of PTA current at 150A

Wear mechanism

The abrasive wear resistance tests performed on the prepared hardfaced layers proceeded in conformity to the procedures outlined in ASTM G65-00. A rubber wheel with quartz sand of grain size 0.297 mm – 0.210 mm was used for this test. A visualization of the sequence of wear has been presented in Fig. 10. Initially, there is removal of tiny amounts of wear debris from the surface as the rubber wheel and quartz sand get into contact with the surface in Fig. 10a. At this stage, the the bulk of the WC particles are positioned slightly below the surface. The surface is moslty composed of the Ni-based matrix. Revolutions from the rubber wheel propel the quartz sand to remove material from the surface as the wear phenomenon gradually approaches the mass of the WC particles. As the quartz sand eventually gets into contact with the WC particles, it gradually smears and begins to wear off the carbides. As the operation proceeds, wear debris rich in carbides form on the surface of the layer (Fig. 10b). This film reduces the friction from the quartz sand and

eventually reduces the wear rate significantly. The position of the bulk of the WC particles away from the surface of the layer depends on the values of PGFR and PTA current. These parameters increase the heat of the system as they increase, causing more melting of the powder particles on the surface. With an increase in the PTA current, the surface of the layer becomes smoother, facilitating the wear rates of the quartz sand on the surface [28,29].

(a)   (b)
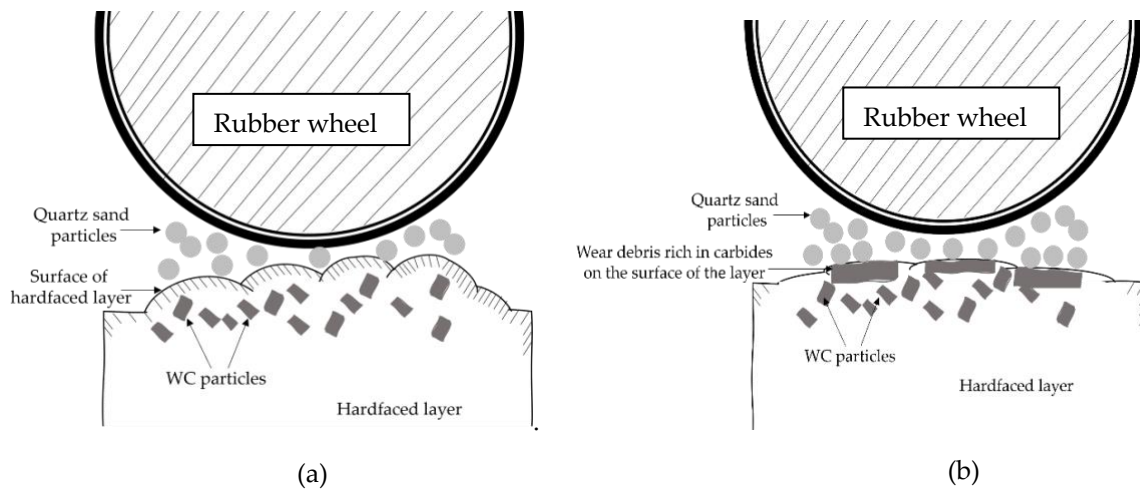
Fig. 10. Wear mechanism of hardfaced layers (a) onset of wear, rubber wheel and quartz sand in contact with the surface of hardfaced layers. Immediate surface is free of WC particles (b) final stage of wear, rubber wheel and quartz sand have worn off WC particle-free surface and now in contact with wear debris rich in carbides, reducing wear friction

Conclusions

1. Powder plasma transferred arc welding (PPTAW) technology was used to prepare hardfaced layers on the surface of a mild steel plate based on the powders of wear-resistant Ni-based matrix with WC reinforced MMCs of composition NiCrSiB+45%WC and NiSiB+60%WC. Relative to wear-resistant steel Hardox 400, the wear resistance of the prepared layers was significantly higher. The introduction of Cr as an alloying element contributed to increasing the hardness and wear resistance of the layers. Coatings were prepared by varying the PPTAW process parameters – PGFR at 1.0 l/min, 1.2 l/min and 1.5 l/m, and plasma arc current at 110A and 150A.

2. Adjustment of the PGFR to slightly higher values had a corresponding increase in the rate of dissolution of the WC particles in the Ni-based matrix, in its microstructure. This resulted in an increase in the hardness of the hardfaced layer, as well as increase in the abrasive wear resistance. However, at higher values of PGFR, there is development of more cracks on the surface of the layers.

3. Increasing the PTA current also increased the amount of heat introduced and absorbed by the particles, creating a larger heat affected zone (HAZ). The hardness of the hardfaced layer was observed to increase, however, this increase in PTA current resulted in a reduction in wear resistance. The higher heat accompanying the increased current resulted in more dissolution of the WC particles into the Ni-based matrix, revealing a much smoother surface with less cracks.

References

1. Fotovvati, B.; Namdari, N.; Dehghanghadikolaei, A. On coating techniques for surface protection: A review. *J. Manuf. Mater. Process*. **2019**, *3*, 28, doi:10.3390/jmmp3010028.
2. Ashby, M.F.; Jones, D.R.H. *Engineering materials 1: an introduction to properties, applications and design*; Elsevier, 2012; Vol. 1; ISBN 0080966659.

3. Kern, W.; Schuegraf, K.K. Deposition technologies and applications: Introduction and overview. In *Handbook of Thin Film Deposition Processes and Techniques*; Elsevier, 2001; pp. 11–43.

4. Branagan, D.J.; Marshall, M.C.; Meacham, B.E. High toughness high hardness iron based PTAW weld materials. *Mater. Sci. Eng. A* **2006**, *428*, 116–123, doi:10.1016/j.msea.2006.04.089.

5. Veinthal, R.; Sergejev, F.; Zikin, A.; Tarbe, R.; Hornung, J. Abrasive impact wear and surface fatigue wear behaviour of Fe–Cr–C PTA overlays. *Wear* **2013**, *301*, 102–108, doi:10.1016/j.wear.2013.01.077.

6. Rohan, P.; Boxanova, M.; Zhang, L.; Kramar, T.; Lukac, F. High speed steel deposited by pulsed PTA-Frequency influence. In Proceedings of the Proceedings to International Thermal Spray Conference, Dusseldorf, Germany; 2017; pp. 404–407.

7. Zikin, A.; Hussainova, I.; Katsich, C.; Badisch, E.; Tomastik, C. Advanced chromium carbide-based hardfacings. *Surf. Coatings Technol.* **2012**, *206*, 4270–4278, doi:10.1016/j.surfcoat.2012.04.039.

8. Skowrońska, B.; Sokołowski, W.; Rostamian, R. Structural investigation of the Plasma Transferred Arc hardfaced glass mold after operation. *Weld. Technol. Rev.* **2020**, *92*, 55–56, doi:10.26628/wtr.v92i3.1109.

9. Bober, M.; Senkara, J. Comparative tests of plasma-surfaced nickel layers with chromium and titanium carbides. *Weld. Int.* **2016**, *30*, 107–111, doi:10.1080/09507116.2014.937616.

10. Niu, J.; Guo, W.; Guo, M.; Lu, S. Plasma application in thermal processing of materials. *Vacuum* **2002**, *65*, 263–266, doi:10.1016/S0042-207X(01)00430-4.

11. Mendez, P.F.; Barnes, N.; Bell, K.; Borle, S.D.; Gajapathi, S.S.; Guest, S.D.; Izadi, H.; Gol, A.K.; Wood, G. Welding processes for wear resistant overlays. *J. Manuf. Process.* **2014**, *16*, 4–25, doi:10.1016/j.jmapro.2013.06.011.

12. Kesavan, D.; Kamaraj, M. The microstructure and high temperature wear performance of a nickel base hardfaced coating. *Surf. coatings Technol.* **2010**, *204*, 4034–4043, doi:10.1016/j.surfcoat.2010.05.022.

13. Szala, M.; Hejwowski, T.; Lenart, I. Cavitation erosion resistance of Ni-Co based coatings. *Adv. Sci. Technol. Res. J.* **2014**, *8*, doi:10.1016/j.wear.2011.05.012.

14. Mandal, S.; Kumar, S.; Bhargava, P.; Premsingh, C.H.; Paul, C.P.; Kukreja, L.M. An experimental investigation and analysis of PTAW process. *Mater. Manuf. Process.* **2015**, *30*, 1131–1137, doi:10.1080/10426914.2014.984227.

15. Qi, C.; Zhan, X.; Gao, Q.; Liu, L.; Song, Y.; Li, Y. The influence of the pre-placed powder layers on the morphology, microscopic characteristics and microhardness of Ti-6Al-4V/WC MMC coatings during laser cladding. *Opt. Laser Technol.* **2019**, *119*, 105572, doi:10.1016/j.optlastec.2019.105572.

16. Ye, T.; Ju, J.; Fu, H.; Ma, S.; Lin, J.; Lei, Y. Effects of Chromium Content on Microstructure, Hardness, and Wear Resistance of As-Cast Fe-Cr-B Alloy. *J. Mater. Eng. Perform.* **2018**, *28*, 6427–6437, doi:10.1007/s11665-019-04369-5.

17. Huang, S.W.; Samandi, M.; Brandt, M. Abrasive wear performance and microstructure of laser clad WC/Ni layers. *wear* **2004**, *256*, 1095–1105, doi:10.1016/S0043-1648(03)00526-X.

18. Czupryński, A.; Żuk, M. Matrix Composite Coatings Deposited on AISI 4715 Steel by Powder Plasma-Transferred Arc Welding. Part 3. Comparison of the Brittle Fracture Resistance of Wear-Resistant Composite Layers Surfaced Using the PPTAW Method. *Materials (Basel).* **2021**, *14*, 6066, doi:10.3390/ma14206066.

19. Xu, H.; Huang, H.; Liu, Z. Influence of Plasma Transferred Arc Remelting on Microstructure and Properties of PTAW-Deposited Ni-Based Overlay Coating. *J. Therm. Spray Technol.* **2021**, *30*, 946–958, doi:10.1007/s11666-021-01183-1.

20. Li, G.L.; Ma, J.L.; Wang, H.D.; Kang, J.J.; Xu, B.S. Effects of argon gas flow rate on the microstructure and micromechanical properties of supersonic plasma sprayed nanostructured Al 2 O 3 -13 wt.%TiO 2 coatings. *Appl. Surf. Sci.* **2014**, *311*, 124–130, doi:10.1016/j.apsusc.2014.05.025.

21. El-Mahallawi, I.; Abdel-Karim, R.; Naguib, A. Evaluation of effect of chromium on wear performance of high manganese steel. *Mater. Sci. Technol.* **2001**, *17*, 1385–1390, doi:10.1179/026708301101509340.

22. Wilden, J.; Bergmann, J.P.; Frank, H. Plasma transferred arc welding—modeling and experimental optimization. *J. Therm. spray Technol.* **2006**, *15*, 779–784, doi:10.1361/105996306X146767.

23. Yibo, X.; Dongqing, L.; Zhizhen, Z.; Jianjun, L.; Tiantian, D. The Effect of Different Arc Currents on the Microstructure and Tribological Behaviors of Cu. **2018**, doi:10.3390/met8120984.

24. Czupryński, A. Microstructure and Abrasive Wear Resistance of Metal Matrix Composite Coatings Deposited on Steel Grade AISI 4715 by Powder Plasma Transferred Arc Welding Part 1. Mechanical and Structural Properties of a Cobalt-Based Alloy Surface Layer Reinforced with P. *Materials (Basel).* **2021**, *14*, 2382, doi:10.3390/ma14112805.

25. Fernandes, F.; Lopes, B.; Cavaleiro, A.; Ramalho, A.; Loureiro, A. Effect of arc current on microstructure and wear characteristics of a Ni-based coating deposited by PTA on gray cast iron. *Surf. Coatings Technol.* **2011**, *205*, 4094–4106, doi:10.1016/j.surfcoat.2011.03.008.
26. Paes, R.M.G.; Scheid, A. Effect of deposition current on microstructure and properties of CoCrWC alloy PTA coatings. *Soldag. Inspeção* **2014**, *19*, 247–254, doi:10.1590/0104-9224/si1903.07.
27. Om, H.; Pandey, S. Effect of heat input on dilution and heat affected zone in submerged arc welding process. *Sadhana* **2013**, *38*, 1369–1391, doi:10.1007/s12046-013-0182-9.
28. Bansal, A.; Zafar, S.; Sharma, A.K. Microstructure and abrasive wear performance of Ni-WC composite microwave clad. *J. Mater. Eng. Perform.* **2015**, *24*, 3708–3716, doi:10.1007/s11665-015-1657-0.
29. Qiao, L.; Wu, Y.; Hong, S.; Long, W.; Cheng, J. Wet abrasive wear behavior of WC-based cermet coatings prepared by HVOF spraying. *Ceram. Int.* **2021**, *47*, 1829–1836, doi:10.1016/j.ceramint.2020.09.009.